

## Urethanes and Polyurethanes Bearing Furan Moieties. 4. Synthesis, Kinetics, and Characterization of Linear Polymers

Sami Boufi, Mohamed Naceur Belgacem, Joel Quillerou, and Alessandro Gandini\*

Matériaux Polymères, Ecole Française de Papeterie et des Industries Graphiques (INPG), BP 65, 38402 St. Martin d'Hères, France

Received May 25, 1993; Revised Manuscript Received August 31, 1993\*

**ABSTRACT:** The synthesis and characterization of a novel family of linear polyurethanes is reported. The original feature stems from the use of *furanic* monomers, either as diols, or as diisocyanates or both. The kinetics of these systems followed the classical second-order behavior with rate constants which showed a marked influence of steric and electronic factors linked to the specific structures of both types of furanic monomers. All polyurethanes had regular structures and fairly high molecular masses, viz. around 10000. A careful analysis of their glass transition temperatures made it possible to establish clear-cut correlations as a function of the position and number of furan rings in the polymer repeat unit. Their thermal degradation gave rise to considerable amounts of carbonaceous residues, which was more, the higher the proportion of furan rings in the structure.

### Introduction

Our laboratory has been engaged for several years in research dealing with the exploitation of vegetable biomass as a source of new monomers and polymers.<sup>1</sup> The renewable character of these resources is an important factor in this strategy. The other interesting aspect stems from the originality of certain chemical and physical properties associated with these structures. In particular, furanic monomers and polymers derived from pentoses and hexoses (sugars and polysaccharides) constitute a peculiar domain of macromolecular science characterized by rather unique features in many respects, as we have shown in numerous studies on both polyaddition and polycondensation reactions and on the products arising from them.<sup>2</sup>

Polyurethanes containing furan rings are a recent addition to our comprehensive study of furanic polymers. As we pointed out previously, the fact that this topic had not received much attention, particularly in terms of the synthesis of furanic diisocyanates and the stability of furanic urethanes,<sup>3-5</sup> prompted us to carry out a preliminary detailed study on the preparation and characterization of several monofunctional model compounds and new monomers, both alcohols and isocyanates, including an assessment of their stability.<sup>3</sup> This was followed by an investigation of the kinetics of formation of mono- and diurethanes bearing furan rings and the study of their structure and stability.<sup>4,5</sup>

The results of this progressive approach clearly indicated that many model structures were devoid of problems both at the synthetic stage (lack of side reactions) and with regard to the stability of reagents and products. The use of furanic difunctional isocyanates and/or diols related to these reliable structures was the next step which provided linear polyurethanes, i.e. the original aim of our enterprise. The present paper reports the first results on a large family of linear furanic polyurethanes.

### Experimental Section

**Monomer Synthesis. Diols.** The syntheses, purification and characterization of 1-(2-furyl)ethylene glycol (1) (mp 13 °C) and 1,2-di(2-furyl)ethylene glycol (2) have already been described.<sup>6</sup> Commercial 2,5-bis(hydroxymethyl)furan (3) was a kind

gift from QO Chemicals Europe and was purified by recrystallization from a tetrahydrofuran (THF) solution or by vacuum sublimation. The latter technique provided a purer compound, mp 70 °C, which was therefore used in the polymerization reactions. 3,4-Bis(hydroxymethyl)furan (4) was prepared by saponification of commercial 3,4-bis(acetoxymethyl)furan and purified by vacuum distillation onto CaH<sub>2</sub> (bp 80 °C/0.05 Torr). The resulting colorless liquid had a melting point of 19 °C. Bis[5-(hydroxymethyl)-2-furfuryl] ether (5) was prepared by reducing the corresponding dialdehyde (generously supplied by the Laboratoire de Chimie des Agroressources, LCA, of Toulouse National Polytechnic Institute) with LiAlH<sub>4</sub> in THF at 0 °C. After conventional workup, the product was recrystallized from dry ether: mp 94 °C. The FTIR spectra of these diols were consistently in tune with the expected structure. Their <sup>1</sup>H-NMR spectral features, assembled in Table I, clearly confirmed this conclusion.

Aliphatic diols were also used. High-purity dry commercial ethylene glycol (6) was utilized as supplied whereas commercial 1,4-butanediol (7) was purified by distillation and collected over CaH<sub>2</sub>.

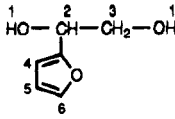
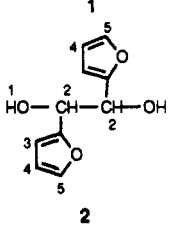
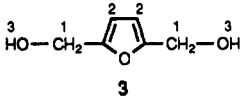
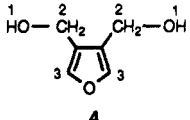
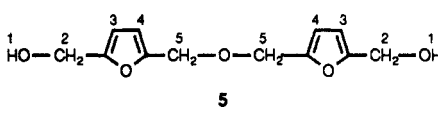
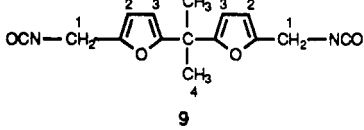
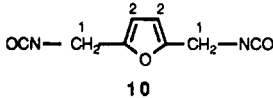
**Diisocyanates.** 2,5-Furyl diisocyanate was not used because of its excessive sensitivity to resinification and because the urethanes derived from it were not very stable.<sup>5</sup> Instead, we called upon its homologue bearing methylene groups between the ring and each NCO function, viz. 2,5-furfuryl diisocyanate (8), which was synthesized from 2,5-bis(aminomethyl)furan (kindly provided by LCA) using bis(trichloromethyl) carbonate (triphosgene)<sup>6</sup> in chlorobenzene to insert the CO moiety. It was purified by thin-film high vacuum distillation, bp 65 °C/2 Torr. 5,5'-Isopropylidenebis(2-furfuryl isocyanate) (9) and its *n*-butyl homologue 10 were the other furanic diisocyanates used in this work. They were synthesized from the corresponding amines following a published procedure,<sup>7</sup> but using triphosgene as functionalizing agent.<sup>3,5,6</sup> They were both purified to 99.5% (GLC) by thin-film vacuum distillation: 9, mp 17 °C. The FTIR spectra of these furanic diisocyanates were in good agreement with the expected structures, and this was confirmed by <sup>1</sup>H-NMR spectroscopy as reported in Table I.

Two typical commercial diisocyanates were also employed, viz. diphenylmethane diisocyanate (11), purified by recrystallization from hexane, and high-purity hexamethylene diisocyanate (12), used as supplied.

**Other Reagents and Solvents.** The polymerization solvents used were dimethylformamide (DMF), dimethylacetamide (DMA), and 1,4-dichlorobenzene (DCB). All were pure anhydrous commercial samples. Whenever a polymerization catalyst was deemed necessary, commercial dibutyltin dilaurate was used as received. Commercial diisopropylamine (used as such) and *tert*-butylmethanol (purified by sublimation under nitrogen after

\* Abstract published in *Advance ACS Abstracts*, October 15, 1993.

Table I.  $^1\text{H}$  NMR Data and Melting Point of Furanic Diols and Diisocyanates

diols and diisocyanates	$\delta$ (ppm) (number of proton, multiplicity)	$T_m$ (deg)
	H <sub>1</sub> 4.1 (1H, s), H <sub>2</sub> 4.72 (1H, t), H <sub>3</sub> 3.72 (2H, d), H <sub>4</sub> 6.23 (1H, m), H <sub>5</sub> 6.3 (1H, m), H <sub>6</sub> 7.32 (1H, m)	13
	H <sub>1</sub> 4.2 (1H, s), H <sub>2</sub> 4.98 (1H, s), H <sub>3</sub> 6.2 (1H, m), H <sub>4</sub> 6.31 (1H, m), H <sub>5</sub> 7.32 (1H, m)	61
	H <sub>1</sub> 4.45 (2H, s), H <sub>2</sub> 6.2 (2H, s), H <sub>3</sub> 4.25 (1H, s)	70
	H <sub>1</sub> 4.4 (1H, t), H <sub>2</sub> 4.52 (4H, d), H <sub>3</sub> 7.42 (2H, s)	19
	H <sub>1</sub> 4.27 (1H, t), H <sub>2</sub> 4.48 (2H, d), H <sub>3</sub> 6.23 (1H, m), H <sub>4</sub> 6.31 (1H, m), H <sub>5</sub> 4.42 (2H, s)	94
	H <sub>1</sub> 4.29 (2H, s), H <sub>2</sub> 5.95 (1H, d), H <sub>3</sub> 6.14 (1H, d), H <sub>4</sub> 1.63 (6H, s)	17
	H <sub>1</sub> 4.45 (2H, s), H <sub>2</sub> 5.28 (2H, s)	

drying over  $\text{CaH}_2$ ) served as NMR enhancing reactive probes for the NCO-terminated polymers.

**Polymerizations and Polymer Characterizations. Kinetic Study.** Equimolar amounts of diol and diisocyanate in solution were mixed under stirring in a flask kept inside a nitrogen glove box at constant temperature to give an initial functional concentration of 0.2 M. Samples were withdrawn periodically, introduced into an IR 50  $\mu\text{m}$ -path cell and examined on an FTIR spectrometer. The optical density of the NCO peak around 2250  $\text{cm}^{-1}$  constituted the relevant variable which was followed as a function of reaction time.

**Polymer Synthesis and Characterization.** Typically, the two monomers in DMA were mixed in a flask kept in a nitrogen glove box to give a monomer concentration 0.5 M, and 0.2% (mol/mol NCO) of catalyst was then added. The temperature was raised to 70  $^\circ\text{C}$  under stirring and the reaction allowed to proceed for 24 h. The clear viscous solution obtained was poured into an excess of ether to precipitate the polyurethane formed. These polymers, in the form of powders or elastomers were filtered and vacuum-dried to constant weight. The characterization of the products involved FTIR and NMR spectroscopy, elemental analysis, molecular mass determination by viscosimetry, GPC, end-group enhancement and light scattering, DCS, TGA, and optical microscopy.

## Results and Discussion

A number of preliminary qualitative runs followed by a rough polymer characterization indicated that polymerizations occurred without any appreciable drawbacks or side reactions and that the polyurethanes bore the expected structure. These observations confirmed the conclusions drawn from all previous studies on model compounds.<sup>3-5</sup>

**Kinetics of Polycondensation.** First of all the validity of Lambert-Beer law applied to the NCO peak around 2250  $\text{cm}^{-1}$  was verified experimentally up to a concentration of 0.5 M. The decrease in optical density of this peak with time could therefore be correlated directly to the actual concentration of the isocyanate functions. The kinetic data obtained were treated according to a second-order behavior, namely:

$$-d[\text{NCO}]/dt = k_2[\text{NCO}][\text{OH}]$$

Since in our context  $[\text{NCO}] = [\text{OH}]$  throughout the polycondensation reaction,

$$-d[\text{NCO}]/dt = k_2[\text{NCO}]^2$$

and therefore:

$$1/[\text{NCO}] - 1/[\text{NCO}]_0 = k_2 t$$

Replacing the NCO concentration by the value of the optical density  $A$  of the NCO peak divided by the product of the extinction coefficient and the optical path length  $l$ , one can write:

$$(A_0 - A)/A = k_2[\text{NCO}]_0 t$$

Figure 1 shows the progression of the IR NCO peak with time for a typical polymerization. Figure 2 gives the corresponding conversion vs time and second-order plots. The IR technique adopted here was reliable up to about 90% conversion. The linearity of the second-order plots was always good up to about 60% and often up to 80%. In all instances, a positive deviation was observed at higher

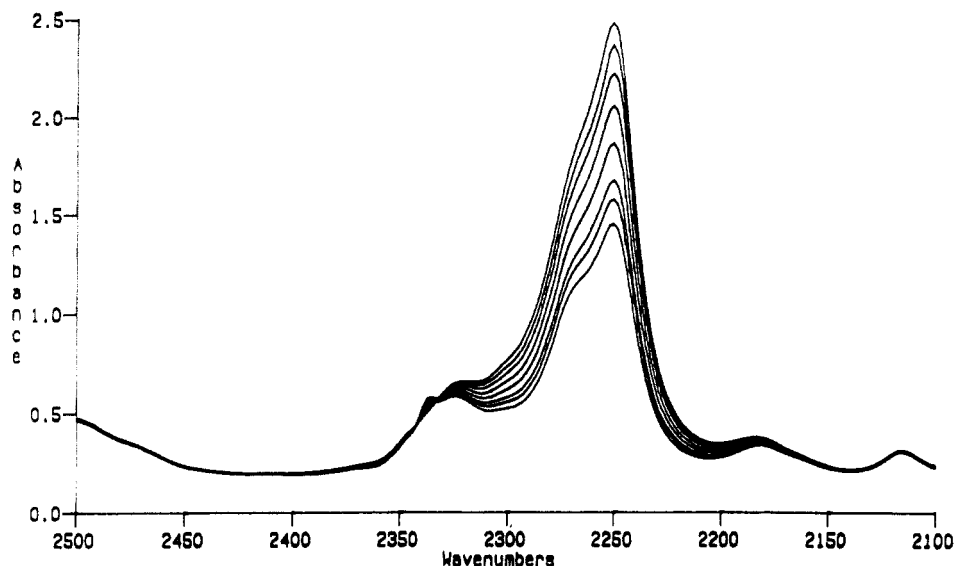


Figure 1. Typical evolution of NCO band with reaction time.

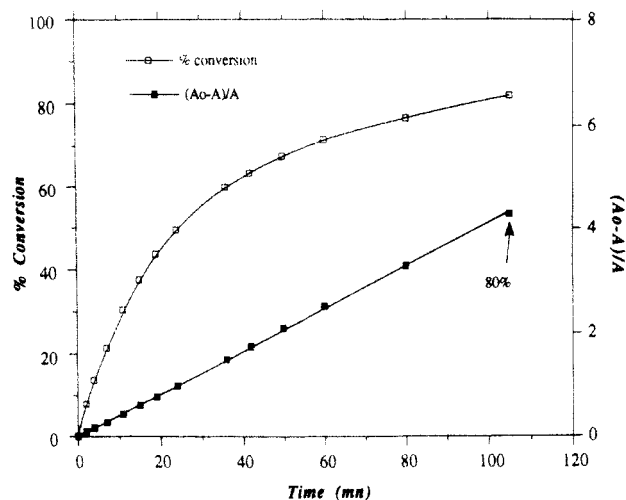


Figure 2. Conversion and second-order plot for the reaction of diisocyanate 11 with diol 3 in DMF at 23 °C.

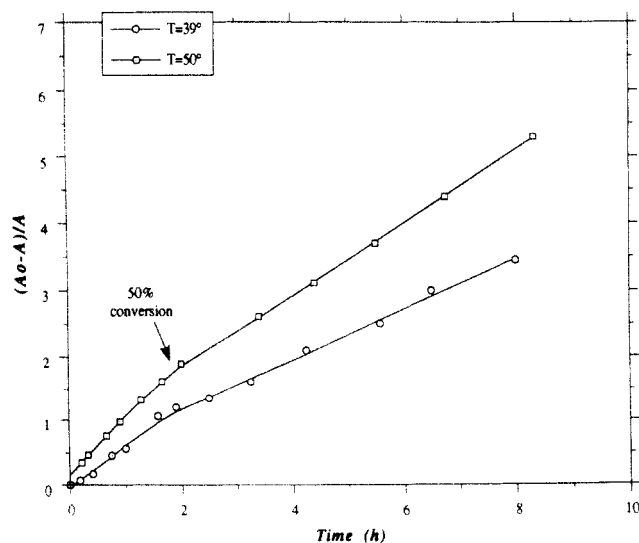


Figure 3. Second-order plot for the reaction of diisocyanate 11 with diol 1 in DMF at 39 °C and 50 °C.

conversions and this phenomenon was more pronounced the higher the polymerization temperature, as indicated in Figure 3. This behavior has already been observed in other polyurethane syntheses<sup>8,9</sup> and suggests an autocatalytic effect induced by the urethane moieties or the

Table II. Second-Order Rate Constants for the Reaction between Diols and Diisocyanates 11 with  $[\text{NCO}]_0 = [\text{OH}]_0 = 0.2 \text{ mol/L}$ , Conducted in DMF, at Different Temperatures

diols	temp (deg)	$k_2 \cdot 10^4$ (L mol <sup>-1</sup> s <sup>-1</sup> )	domain of validity (%)	$E_a$ (kJ mol <sup>-1</sup> )
<chem>Oc1ccccc1COc2ccccc2CO</chem> <b>2</b>	80	8.35		
	70	5.5	55	
	60	3.2	60	
	23	0.4	70	46
<chem>Oc1ccc(O)cc1</chem> <b>3</b>	23	155	80	
	8	75	85	
	2	61	85	32
<chem>Oc1ccc(O)cc1</chem> <b>4</b>	23	30.5	80	
<chem>OCCCO</chem> <b>6</b>	23	18.6	75	
<chem>OCCCOCCCO</chem> <b>7</b>	23	80	85	

consumption of NCO groups in side reactions like the formation of allophanates.

Table II gives the values of the second-order constants and some activation energies referred to the reactions based on diisocyanate 11 and various diols including aliphatic ones, used for the sake of comparison with the furanic structures. The domain of second-order behavior extended to 70–85% conversion at, or below, room temperature and decreased to about 50% when the polymerization temperature was raised to 70–80 °C. As for the relative values of  $k_2$ , several comments seem appropriate: (i) with aliphatic diols, the higher reactivity of 7 with respect to 6 stems from the well-known importance of intramolecular hydrogen bonding in the latter,<sup>10</sup> which obviously reduces the reactivity of its hydroxy groups toward isocyanate functions; (ii) a comparison of the  $k_2$  for 7 and 3 reveals that the  $\text{CH}_2\text{OH}$  groups attached to the C2 and C5 positions of the furan ring cannot interact to any appreciable extent to form intramolecular hydrogen bonds, either between themselves, or with the ring oxygen atom and therefore

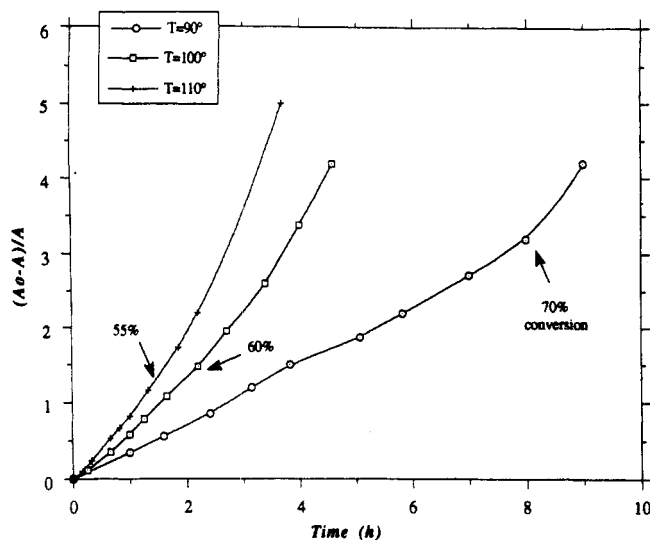


Figure 4. Second-order plot for the reaction of diisocyanate 9 with diol 3 in DMF at various temperatures.

Table III. Second-Order Rate Constants for the Reaction between Diols and Furanic Diisocyanates 9 with  $[NCO]_0 = [OH]_0 = 0.2 \text{ mol/L}$ , Conducted in DMF, at Different Temperatures

diols	temp (deg)	$k_2 \cdot 10^4$ ( $\text{L mol}^{-1} \text{s}^{-1}$ )	domain of validity (%)	$E_a$ (kJ $\text{mol}^{-1}$ )
<chem>OCC1=CC=C(O)C=C1</chem> 1	120	19	40	37
	110	13.3	50	
	90	6.4	60	
<chem>OCC1=CC=C(O)C=C1</chem> 2	120	8.9	45	66
	110	5.2	55	
	100	3	60	
	90	1.7	70	
<chem>OCC1=CC=C(O)C=C1</chem> 3	110	11	55	43
	100	7.8	60	
	90	5.5	70	
	70	2.6	80	
<chem>OCC1=CC=C(O)C=C1</chem> 4	90	6.2	65	
<chem>OCC1=CC=C(O)C=C1</chem> 6	90	7.3	70	

Table IV. Second-Order Rate Constants for Bulk Reactions at Room Temperature without Catalyst

PU	$k_2 \cdot 10^4$ ( $\text{L mol}^{-1} \text{s}^{-1}$ )	domain of validity (%)
9 + 6	15	20
9 + 1	3.5	20
9 + 4	35	25
12 + 6	0.58	30

they exhibit a very marked reactivity; (iii) the previous conclusion is corroborated by the fact that diol 4 is much less reactive than 3 and indeed considerably less reactive than 7 precisely because the position of the two  $\text{CH}_2\text{OH}$  groups is now particularly favorable to mutual hydrogen bonding, almost to the same extent as 6; (iv) diol 2 is very sluggish because of the concomitant effect of steric hindrance introduced by the furan rings upon each secondary OH function and the occurrence of hydrogen bonding between them.

We only measured the activation energies for the two limiting situations, viz. with 2 and 3. The difference is in

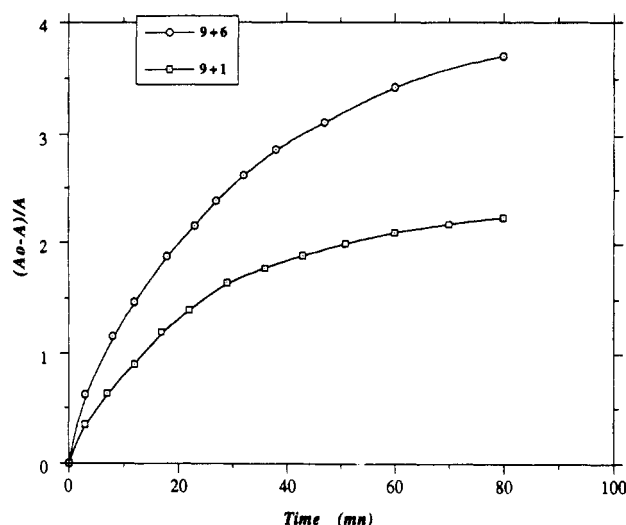


Figure 5. Second-order plot for the bulk reaction of diisocyanate 9 with diols 1 and 6 at room temperature.

Table V. Elemental Analyses of Some Furanic Polyurethanes

polyurethane	C		H		O		N	
	calcd	found	calcd	found	calcd	found	calcd	found
11 + 1	66.5	65.8	4.82	5.4	21	20.7	7.5	8.1
11 + 4	66.5	65.5	4.82	5.5	21	20.8	7.5	8.5
9 + 4	60.7	59.8	6.7	6	27	27	5.51	7.2
9 + 1	60.7	60.6	6.7	7	27	26.3	5.51	6.1
12 + 1	56.7	56.5	6.8	7	27	26.4	9.5	10

the right direction, but its magnitude is relatively modest. The fact of having used DMF as solvent certainly favored the reaction in general because of its well-known catalytic role<sup>11,12</sup> and thus reduced the activation energies as a whole, e.g. as compared with the values obtained previously for the formation of monourethanes in nitromethane,<sup>4</sup> but also decreased the gap between activation energies for different compounds. In the present study we measured  $k_2$  with 3 + 11 in DMF at room temperature and dichlorobenzene at 100 °C and found a dramatic decrease with the latter solvent even if the reaction was conducted at much higher temperature, viz. from  $1.6 \times 10^{-2}$  (23 °C) to  $2.3 \times 10^{-3} \text{ L mol}^{-1} \text{s}^{-1}$  (100 °C). This confirms the positive role of DMF in the present context.

The kinetic behavior of asymmetric diol 1 which bears a primary and a secondary OH is shown in Figure 4. One can clearly discern two linear portions with a decrease in slope at about 50% conversion. This is obviously associated with the different reactivity of the hydroxy groups which turns out to be close to a factor of 2, as indicated in Table II. The overall activation energy is intermediate between those obtained with primary and secondary symmetric diols, respectively.

Table III reports a similar set of kinetic results, but referred to the furanic diisocyanate 9. On the whole its reactivity was much lower than that of the aromatic monomer 11 and therefore the polymerizations were carried out at higher temperatures. As a consequence, the positive deviation with respect to the linear second-order behavior occurred at rather low conversions. It appears that above about 80 °C the extent of intramolecular hydrogen bonding becomes negligible with all the diols tested since the  $k_2$  values referred to primary OH functions became very similar, and only the steric effect played a major role as shown by the 3–4-fold drop in  $k_2$  with diol 2. The activation energies point to the same trend, but they were somewhat higher than with the

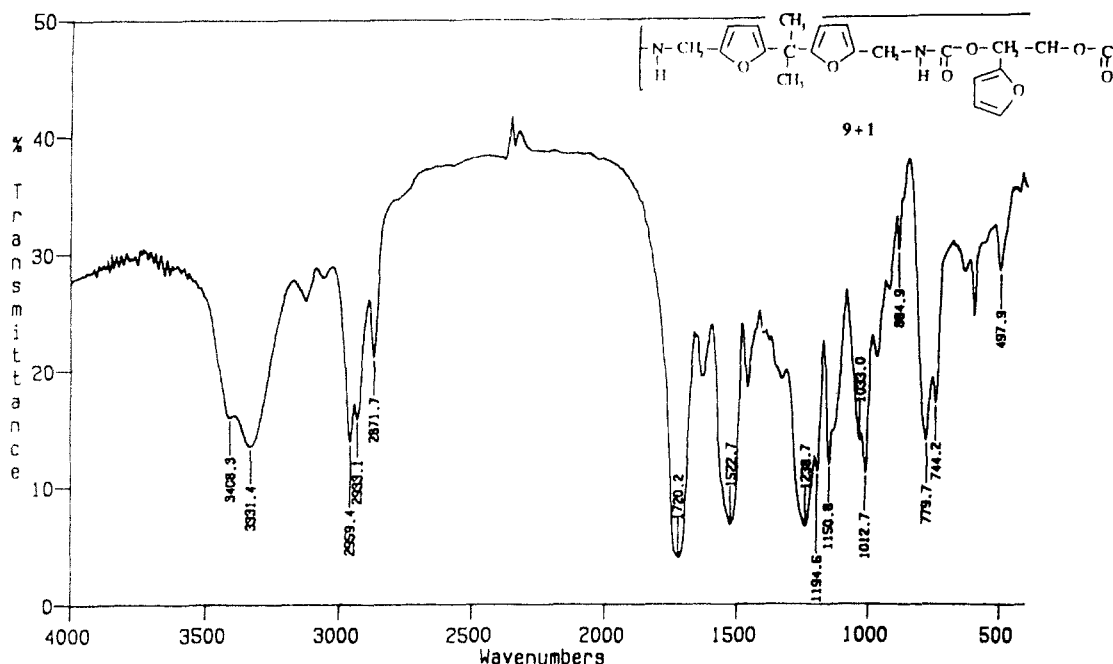


Figure 6. FTIR spectrum (KBR pellet) of polyurethane 11 + 3.

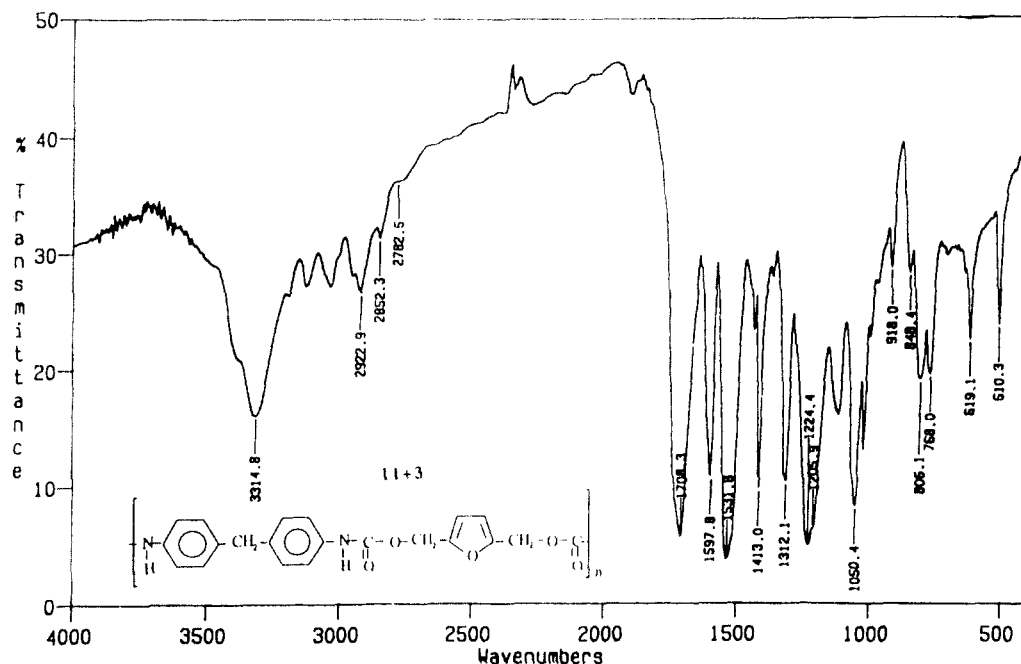


Figure 7. FTIR spectrum (KBR pellet) of polyurethane 9 + 1.

aromatic diisocyanate (see Table II). The latter difference together with the considerable overall decrease in  $k_2$  with the furanic diisocyanate can be explained by the fact that whereas in structure 11 the NCO function is bound directly to the aromatic ring and this conjugation enhances its reactivity, in structure 9 a methylene group separates the isocyanate moiety from the furan heterocycle. However, the diisocyanate 9 must not be considered as equivalent in reactivity to an aliphatic structure. We measured  $k_2$  at 100 °C in dichlorobenzene with diol 3 and diisocyanates 11, 9, and 12 and found values of  $2.3 \times 10^{-3}$ ,  $3 \times 10^{-4}$ , and  $3.5 \times 10^{-5} \text{ L mol}^{-1} \text{ s}^{-1}$ , respectively, which show clearly that the furanic diisocyanate is more reactive than the aliphatic one. This difference is attributed to an inductive effect of the heterocycle onto the NCO group through the methylene bridge. As for the relative reactivity of the aromatic and furanic diisocyanates, one notices that it is much more pronounced in DMF (a factor of more than

100) than in dichlorobenzene (a factor of about 7). This confirms the catalytic role of the former solvent.

The kinetics of some reactions conducted in bulk were also followed, and in these experiments the mixture of monomers *without catalyst* was prepared and rapidly placed in the IR cell which was the actual reaction site at room temperature since the high monomer concentrations rendered the polymerization much faster and sampling was not viable. The spectra were therefore taken repetitively from the polymerizing mixture within the cell. Table IV shows the results obtained. Contrary to the general behavior in solution, these reactions tended to *slow down* considerably with respect to second-order kinetics, as shown in Figure 5. This feature is attributed to the rapid increase in viscosity of the medium which obviously limited macromolecular mobility thus rendering the reactions diffusion controlled. This phenomenon is well documented in bulk polymerizations involving polyurethanes.<sup>13,14</sup>

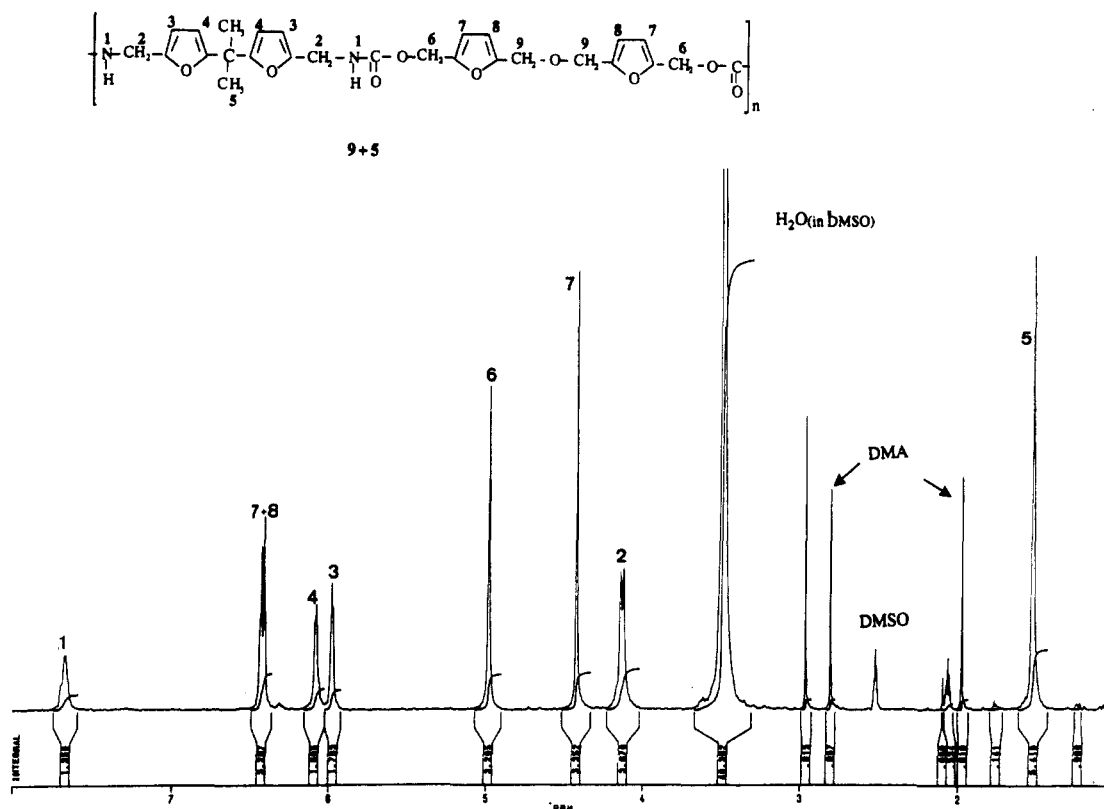


Figure 8.  $^1\text{H}$ -NMR spectrum (30 MHz) of polyurethane 9 + 5 in  $\text{DMSO}-d_6$ .

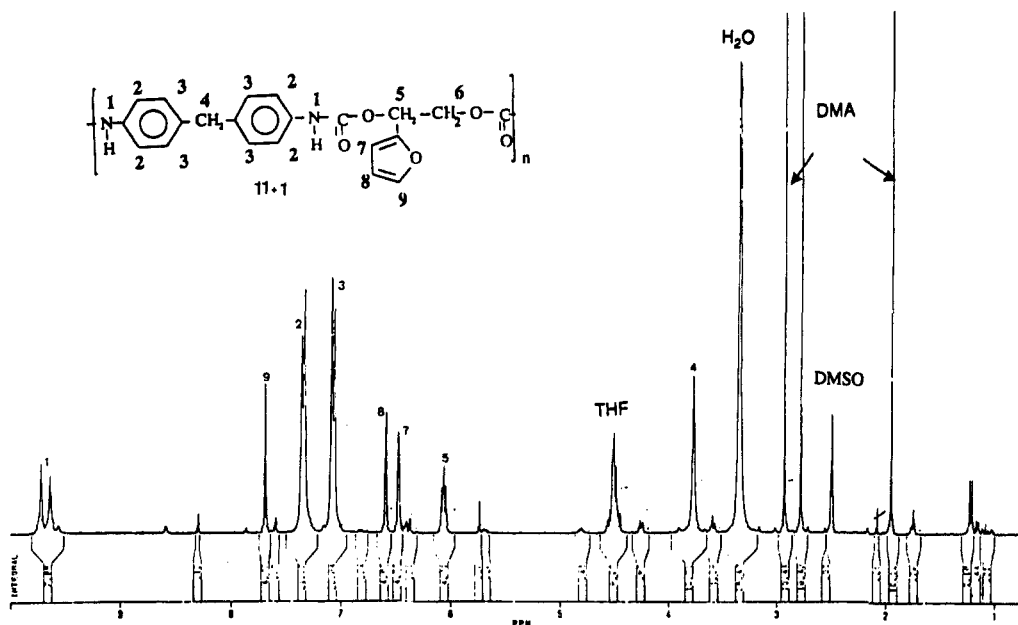


Figure 9.  $^1\text{H}$ -NMR spectrum (300 MHz) of polyurethane 11 + 1 in  $\text{DMSO}-d_6$ .

A comparison of the  $k_2$  values shows a behavior which is very similar to that of room temperature reactions in solution with the aromatic diisocyanate 11 (see Table II). More specifically, the joint effects of intramolecular hydrogen bonding and steric problems related to the diols are clearly present with these systems comprising a furanic diisocyanate because the reaction temperature here is much lower than in the corresponding systems in solution (see Table III). Also, one finds again the notable difference in reactivity between the furanic diisocyanate 9 and the aliphatic structure 12, an observation which confirms that the separation of the NCO function from the heterocycle by a methylene group is not sufficient to eliminate electronic communication through inductive effects, i.e. that 9 must not be viewed as an "aliphatic diisocyanate".

In conclusion to this kinetic study it can be said that (i) no anomaly with respect to well-documented aliphatic and aromatic polyurethane syntheses were detected thus confirming<sup>3-5</sup> that the presence of the furan rings in either type of monomer does not introduce any perturbing effect during the course of these reactions; (ii) the reactivity of furanic diols follows classical criteria already established with model reactions,<sup>4,5</sup> (iii) the reactivity of the furanic diisocyanates used in this work is intermediate between those of aliphatic and aromatic counterparts, contrary to the results on model systems<sup>5</sup> for which compound 9 had displayed a reactivity two to three times higher than that of compound 11. We have no valid explanation of this quantitative change in behavior. The present results on polymerization systems show the same trend as those

Table VI. <sup>1</sup>H NMR Data of Furanic Polyurethanes

	$H_1$ 7.71 (t), $H_2$ 4.1 (d), $H_3$ - $H_4$ 5.95-6.05 (d), $H_5$ 1.5 (s), $H_6$ 5.9 (t), $H_7$ 4.3 (d), $H_8$ - $H_9$ 6.5 (d), $H_{10}$ 7.65 (s)
9 + 1	
	$H_1$ 7.71 (t), $H_2$ 4.1 (d), $H_3$ - $H_4$ 5.95-6.05 (d), $H_5$ 1.5 (s), $H_6$ 4.95 (s), $H_7$ 6.5 (s)
9 + 3	
	$H_1$ 7.59 (t), $H_2$ 4.1 (d), $H_3$ - $H_4$ 5.95-6.05 (d), $H_5$ 1.5 (s), $H_6$ 4.92 (s), $H_7$ 7.63 (s)
9 + 4	
	$H_1$ 7.67 (tr), $H_2$ 4.1 (d), $H_3$ - $H_4$ 5.95-6.08 (d), $H_5$ 1.52 (s), $H_6$ 4.96 (s), $H_7$ - $H_8$ 6.4-6.44 (m), $H_9$ 4.41 (s)
9 + 5	
	$H_1$ 7.65 (t), $H_2$ 4.05 (d), $H_3$ - $H_4$ 5.95-6.05 (d), $H_5$ 1.52 (s), $H_6$ 4.12 (s)
9 + 6	
	$H_1$ 7.75 (t), $H_2$ 4.1 (d), $H_3$ - $H_4$ 5.95-6.05 (d), $H_5$ 1.5 (s), $H_6$ 6.1, $H_7$ - $H_8$ 6.3 (d), $H_9$ 7.63 (m)
9 + 2	
	$H_1$ 7.75 (t), $H_2$ 4.1 (d), $H_3$ - $H_4$ 5.95-6.05, $H_5$ 3.97 (t), $H_6$ 1.95, $H_7$ 1.2, $H_8$ 0.85 (d), $H_9$ 5.88 (d), $H_{10}$ 4.32 (d), $H_{11}$ - $H_{12}$ 6.45 (d), $H_{13}$ 7.62 (s)
10 + 1	
	$H_1$ 7.63 (t), $H_2$ 3.31, $H_3$ 1.21, $H_4$ 1.14, $H_5$ 5.88 (d), $H_6$ 4.32 (d), $H_7$ - $H_8$ 6.45 (d), $H_9$ 7.6 (s)
12 + 1	
	$H_1$ 7.63 (t), $H_2$ 3.31, $H_3$ 1.21, $H_4$ 1.14, $H_5$ 5.05 (s), $H_6$ 6.15 (d)
12 + 3	
	$H_1$ 7.75 (t), $H_2$ 4.1 (d), $H_3$ 6.02 (s), $H_4$ 5.05 (s), $H_5$ 6.5 (s)
8 + 3	

Table VI (Continued)

	$H_1$ 7.75 (t), $H_2$ 4.1 (d), $H_3$ 6.06 (s), $H_4$ 5.88 (t), $H_5$ 4.3 (d), $H_6$ - $H_7$ 6.4 (d), $H_8$ 7.63 (m)
	$H_1$ 9.5 (s), $H_2$ 7.3 (d), $H_3$ 7.1 (d), $H_4$ 3.75 (s), $H_5$ 5.07 (s), $H_6$ ; 6.53 (s)
	$H_1$ 9.5 (s), $H_2$ 7.3 (d), $H_3$ 7.1 (d), $H_4$ 3.75 (s), $H_5$ 6.05 (t), $H_6$ - $H_7$ 6.45-6.6 (d), $H_8$ 7.7 (s), $H_9$ 4.5 (d)
	$H_1$ 9.5 (s), $H_2$ 7.3 (d), $H_3$ 7.05 (d), $H_4$ 3.75 (s), $H_5$ 5.01 (s), $H_6$ 7.75 (s)
	$H_1$ 9.5 (s), $H_2$ 7.3 (d), $H_3$ 7.1 (d), $H_4$ 3.75 (s), $H_5$ 6.25 (d), $H_6$ - $H_7$ 6.45-6.57 (d), $H_8$ 7.67 (m)

reported by Cawse et al.<sup>15</sup> who found that 11 was some 10 times more reactive than 9 toward the aliphatic diol 7 in polymerization conditions which however differed substantially from ours.

**Polymer Characterization.** Table V gives some representative analyses of a selection of furanic polyurethanes. They are all in good agreement with the expected structures, and modest differences between calculated and determined compositions are to be attributed to small amounts of solvent or moisture in the products.

The spectroscopic characterization conducted on each polymer involved IR and  $^1\text{H}$ -NMR analyses, whereas  $^{13}\text{C}$  NMR was reserved to a choice of representative structures. All IR spectra bore the characteristic peaks arising from the urethane moiety (at 3400, 1700, and 1260  $\text{cm}^{-1}$  for N-H, C=O and O=C-O, respectively), the absence of the NCO peak around 2250  $\text{cm}^{-1}$ , and the peaks due to the specific structures of the monomers involved. Figures 6 and 7 show typical spectra for a furanic-aromatic and an entirely furanic polyurethane, respectively. In the former, only furanic rings inserted in the main chain through C2-C5 connections are present and this gives rise to their typical peaks between 750 and 1000  $\text{cm}^{-1}$  and in other regions of the spectrum.<sup>16</sup> In the latter, the heterocycles are present both within the main chain and as pendant groups, attached at C2, and the peaks for these mono-substituted rings<sup>16</sup> are also visible in the same regions.

Typical  $^1\text{H}$ -NMR spectra of furanic polyurethanes are given in Figures 8 and 9. The features of these spectra are in complete agreement with the respective expected structures. This was also true of all the other polymers synthesized in this study as indicated in Tables VI which provides the pertinent data. Minor resonances attributed

to structural anomalies or impurities were rare. Figure 10 portrays one of the  $^{13}\text{C}$ -NMR spectra of these products with its structure and corresponding assignments. The fact that each carbon nucleus of the formal structure gave a single resonance in this and all the other spectra constitutes further supporting evidence of the regularity of the polymers prepared.

Molecular masses were the next element of characterization. Different techniques were used to reach reliable conclusions. First, the NCO end groups were made to react with an excess of either isopentanol or diisopropylamine in order to attach a large number of equivalent methyl protons to these sites. The  $^1\text{H}$ -NMR spectra could then be used for counting them in relation to protons belonging to the monomeric units in the chain and thus  $M_n$  ( $\text{DP}_n$ ) could be calculated with a fairly good precision. An example of this approach is shown in Figure 11 which shows the visibility of the nine equivalent protons from the *tert*-butyl group of the reacted alcohol at 0.8 ppm, with respect to all the resonances due to the protons in the chain. Obviously this technique is limited to relatively modest molecular masses, here lower than about 8000 and applies well to polymerizations carried out with a slight excess of NCO functions. The values of  $M_n$  obtained are given in Table VII. The intrinsic viscosities of polyurethane solutions were also determined. The solvent and temperature chosen were those related to published values of  $K$  and  $\alpha$  in the Flory-Huggins equation for the polyurethane formed from 2,4-tolyl diisocyanate and diol 7,<sup>17</sup> viz. a polymer structure as close as could be found to those of the present set of polyurethanes. The  $M_v$  values calculated with these constants are reported in Table VII. Finally, some polymers were also analyzed by light



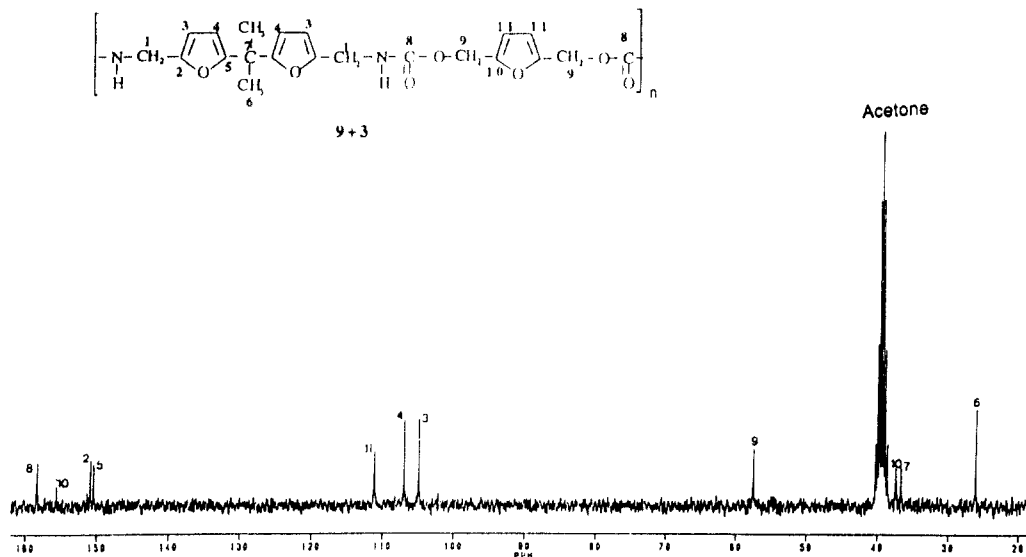


Figure 10.  $^{13}\text{C}$ -NMR spectrum (25 MHz) of polyurethane 9 + 3 in  $\text{DMSO}-d_6$ .

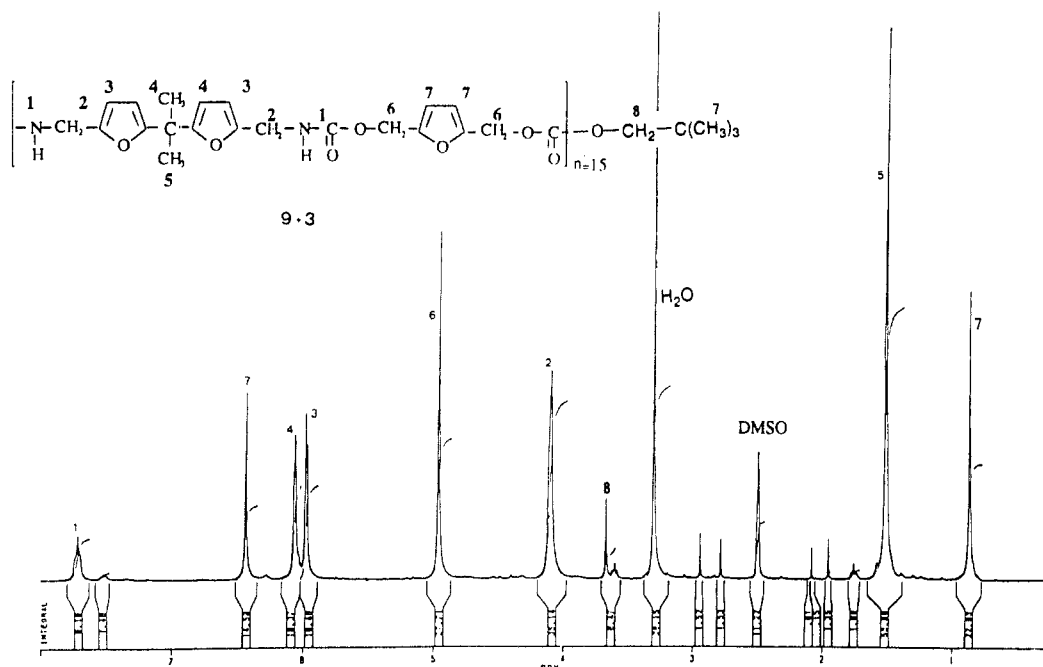


Figure 11.  $^1\text{H}$ -NMR spectrum (300 MHz) of polyurethane 9 + 3 in  $\text{DMSO}-d_6$ , with  $[\text{NCO}]_0/[\text{OH}]_0 = 1.25$ , quenched with *tert*-butylmethanol.

scattering in DMF at 548 nm with a Chromatix laser instrument. Scattered light was measured at three different angles. The  $M_w$  values of the four polyurethanes inspected in this way are also given in Table VII.

A comparison of  $M_n$  and  $M_v$  values shows that for molecular masses below about 8000, the number-average molecular masses are systematically lower than the corresponding viscosity-average values, as expected. For higher polymers the  $M_n$  figures are certainly less accurate and any serious comparison becomes hazardous. The few  $M_w$  values obtained by light scattering are in tune with the expected behavior of a linear polycondensation reaction conducted to high conversions, i.e. they are approximately twice as high as the corresponding  $M_n$ . It can therefore be concluded that the actual figures obtained must be close to the real molecular masses of these polyurethanes. When the syntheses were carried out using near-stoichiometric conditions, the  $M_n$  were close to 10000 which is a respectable figure for such a polycondensation reaction. Table VII also shows values of  $M_n$  and  $M_v$  for nonstoichiometric conditions. The lower figures obtained in these

instances are in close agreement with those calculated. Some of the furanic polyurethanes were submitted to a GPC analysis in THF using a standard series of columns and refractometric plus UV detection. Figure 12 shows two such chromatograms for two polymers possessing the same structure but different molecular masses. The shape of these curves reflects a normal distribution with  $M_w/M_n = 1.8$ , i.e. close to 2, considering the fact that polystyrene was the reference polymer used for the calibration.

The conclusion to this structural investigation is that furanic polyurethanes bearing the expected regular linear monomeric sequences and displaying relatively high molecular masses are readily prepared if the monomers are pure, the reaction medium dry, and the usual care taken to conduct the syntheses. In other words, the presence of furan rings does not influence negatively the structural regularity or the size and size distribution of the macromolecules. These systems behave therefore in a manner entirely similar to that encountered with conventional aliphatic and/or aromatic monomers.

Table VII. Characteristics of Furanic Polyurethanes

polyurethane	$M_n^a$	$M_w^b$	$M_v^c$	$T_g$ (deg)	$T_m$ (deg)	$r^d$
9 + 3	3200	11000	—	45	180	1.25
	5000		8000	55	180	1.11
	—		15000	60		1.05
	2900		—	40		0.9
10 + 1	2500	12000	—	24		1.25
	6000		7000	41		1.11
	—		12000	45		1.05
	—		13000	20	170	1.05
9 + 1	9000	13500	12000	50		1.05
9 + 6	9500		12000	28	156	1.05
9 + 5	—		16500	50	190	1.25
—	3400		—	65	190	1.11
11 + 3	4500	31000	14000	97	207	1.05
—	—		20000	40	185	1.05
11 + 1	6500		10000	74	168	1.05
11 + 2	—		13000	45	175	1.05
11 + 4	7000	13500	8000	45		1.05
9 + 2	—		7000	25	165	1.07
9 + 4	—		8500	30	160	1.07
8 + 3	—		5000	33	185	
8 + 1	8500	9000	6000	17	175	
12 + 3	—		8000			
12 + 1	9000		7000			

<sup>a</sup> From end-group analysis. <sup>b</sup> From light scattering. <sup>c</sup> From intrinsic viscosities. <sup>d</sup>  $[\text{NCO}]_0/[\text{OH}]_0$ .

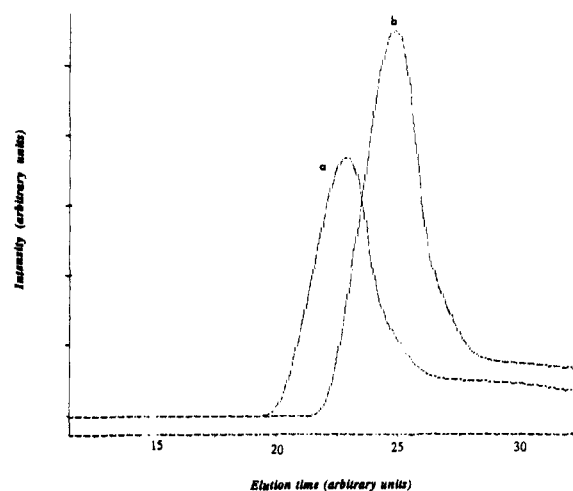


Figure 12. Typical GPC tracing of polyurethane 9 + 1 prepared respectively with (a)  $[\text{NCO}]_0/[\text{OH}]_0 = 1.11$ ; (b)  $[\text{NCO}]_0/[\text{OH}]_0 = 1.05$ .

Table VII collects two more sets of data which concern the thermal transitions of these furanic polyurethanes. The glass-transition temperature of the amorphous polymers is an excellent probe of their chain stiffness. It is therefore instructive to establish some correlations between the  $T_g$  of the present polyurethanes and (i) the relative extent of furanic rings in their structure, but also (ii) their position with respect to the main chain. First of all, the replacement of an aromatic ring for a furanic one, both being planar, results in a decrease in  $T_g$  associated with the smaller size of the heterocycle. On the other hand, the introduction of a furan ring in place of an aliphatic sequence is accompanied by a logical increase in  $T_g$ . These trends apply to situations in which the ring is either within the chain or as a substituent. Thus for example the  $T_g$  of polyvinylfuran is about 60 °C, compared with 5 °C for polypropylene and 100 °C for polystyrene. Polymers 12+3 ( $T_g = 33$  °C), 9+3 ( $T_g = 60$  °C), and 11+3 ( $T_g = 97$  °C) show precisely this trend for variable moieties within the chain as well as the sequence 12+1 ( $T_g = 17$  °C), 9+1 ( $T_g = 20$  °C), and 11+1 ( $T_g = 40$  °C) in which there is also a pendant furan ring. The number of pendant furan rings per monomer unit also affects the  $T_g$  as shown by the increase observed when going from 9+1 ( $T_g = 20$

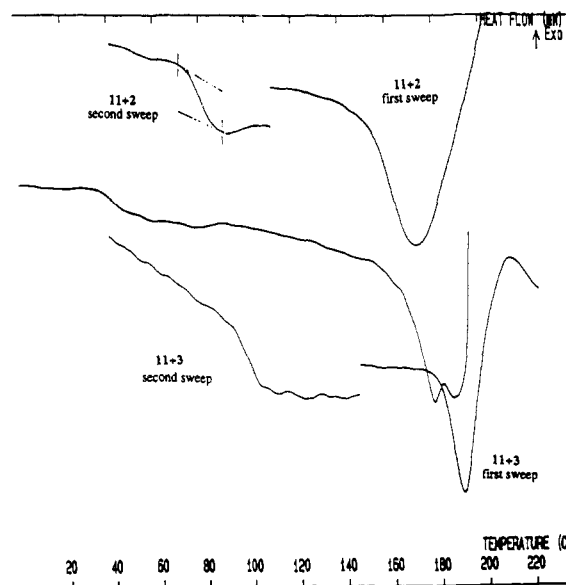


Figure 13. DSC thermograms of some polyurethanes ( $10^\circ \text{ min}^{-1}$ ) after the first sweep. The second sweep corresponds to polymer after quenching with liquid nitrogen.

°C) to 9+2 ( $T_g = 45$  °C), or from 11+1 ( $T_g = 40$  °C) to 11+2 ( $T_g = 74$  °C). In both instances the addition of a further pendant ring introduces an increase in free volume demand, i.e. a higher chain stiffness. All other structural conditions being the same, the position of the ring with respect to the backbone is also an important factor. The maximum stiffness is encountered with the heterocycle enchainment through its C2–C5 sites. The C3–C4 enchainment is less stiffening than the latter, but in turn just a little more rigidifying than the ring as side group attached through its C2 position, as shown in Table VI. A comparison of the series 11+3 ( $T_g = 97$  °C), 11+4 ( $T_g = 45$  °C), and 11+1 ( $T_g = 40$  °C) and of the series 9+3 ( $T_g = 60$  °C), 9+4 ( $T_g = 25$  °C), and 9+1 ( $T_g = 20$  °C) clearly illustrates these trends. The reasons for these variations are associated with both the increasing degree of freedom of movements of the ring and the difficulty of formation of interchain hydrogen bonding with the progressive protuberance of the heterocycle. A similar trend was observed in a previous study on furanic polyamides.<sup>18</sup>

Another notable structural effect on  $T_g$  arises from the introduction of a flexible  $\text{CH}_2\text{OCH}_2$  unit within the polyurethane main chain. Thus, the macromolecular stiffness is reduced when going from polymer 9+3 ( $T_g = 60$  °C) to its homologue 9+5 which bears that spacer ( $T_g = 28$  °C).

All furanic polyurethanes displayed a clear-cut  $T_g$  on the DSC thermograms. Many of them crystallized, but particularly those which had a more symmetric structure. The melting points reported in Table VII were obtained from the characteristic endotherms of the DSC tracings. Figure 13 shows a typical thermogram of a semicrystalline furanic polyurethane with both  $T_g$  and  $T_m$  typical features. The crystalline character was confirmed by the observation, with an optical microscope equipped with polarizers and hot stage, of birefringence and the formation of spherulites from thin films cast from solution.

The thermal degradation of these polymers was investigated by TGA, both under nitrogen and in air. The major feature of all thermograms, as shown in Figure 14, is the onset of weight loss which occurred around 200 °C for the furanic–aromatic and all-furanic polyurethanes and around 250 °C for the furanic–aliphatic structures. This threshold was essentially unchanged when going from nitrogen atmosphere to air and is characteristic of the thermally

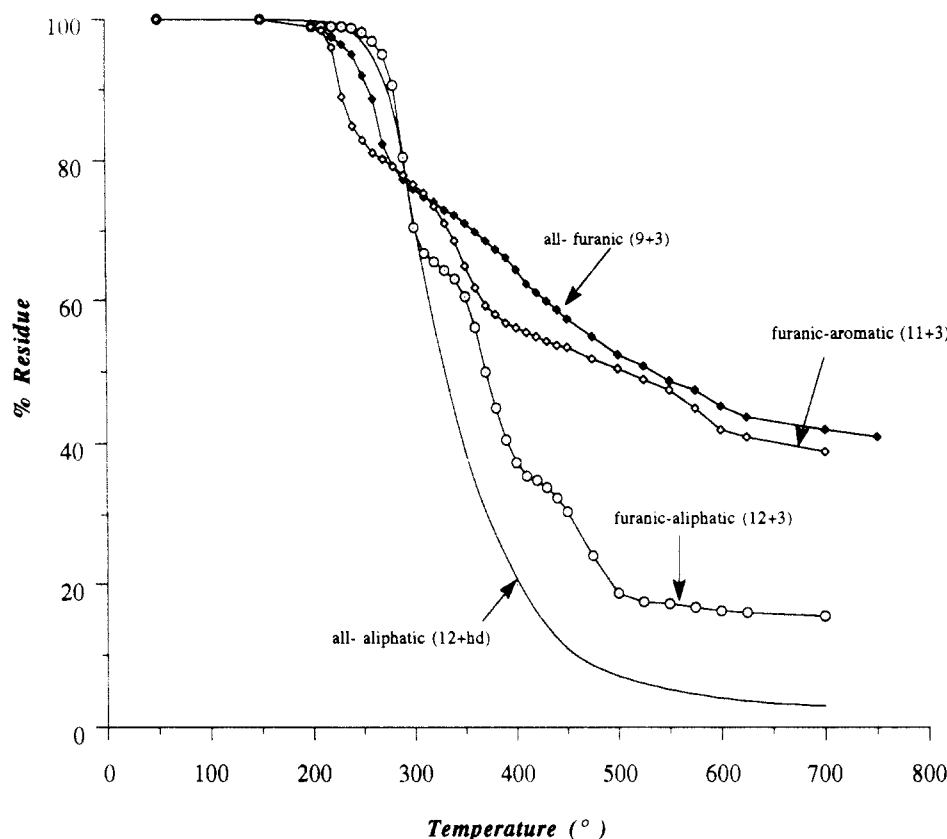


Figure 14. Comparative TGA thermograms under N<sub>2</sub> of polyurethanes of different structures (sweep rate 10° min<sup>-1</sup>).

Table VIII. Residues of Polyurethane at Various Temperatures under Nitrogen

polyurethane	% furan	% residue at 300 °C	% residue at 400 °C	% residue at 700 °C
12 + hd <sup>a</sup>	0	95	20	5
11 + 3	18	75	55	40
11 + 1	18	72	55	39
12 + 3	22	78	38	20
11 + 2	30	63	53	40
9 + 6	38	60	55	40
10 + 3	43	70	62	41
9 + 3	48	76	66	44
9 + 1	48	78	67	47
9 + 2	55	75	65	45

<sup>a</sup> hd: 1,6-hexanediol.

induced reverse reaction of urethane moieties giving back the isocyanate and hydroxy functions. The higher resistance of urethanes from aliphatic isocyanates with respect to aromatic ones is well documented;<sup>19</sup> here, the use of furanic isocyanates leads to a behavior which is close to that of the aromatic counterparts. Figure 14 also shows that in an inert atmosphere the weight loss subsequent to the first threshold is quite dramatic with furanic-aliphatic structures, giving less than 20% residue at 500 °C and much more moderate and spread out with the furanic-aromatic polymers and even more with the totally furanic structures. The tendency of furanic polymers to give carbonaceous residues upon pyrolysis is quite typical and has been thoroughly studied with furfuryl alcohol resins.<sup>20</sup> This feature is illustrated in clear quantitative terms in Table VIII which gives the residues at various temperatures resulting from the pyrolysis under nitrogen of polyurethanes with a growing content of furan moieties. With about 50% of furan rings with respect to the total molecular mass of the repeat unit, the residue at 700 °C reaches almost 50%.

One must therefore distinguish between the thermal fragility intrinsic to the urethane linkages, which is

therefore common to all these polymers albeit with minor temperature variations, and the specific resistance to pyrolysis of the furan heterocycle, which can result in modest rates of volatilization even at high temperatures.

### Concluding Remarks

The present investigation is the first insight into the synthesis and characterization of furanic polyurethanes. The comparative kinetic data obtained have shown that it is possible to correlate satisfactorily the structure of furanic diols and diisocyanates with their reactivity and thus formulate monomer combinations adapted to different situations. The set of structures prepared is sufficiently wide to justify the general conclusion that this new family of polymers is a respectable addition to those already known, viz. the traditional aliphatic and aromatic polyurethanes. The interests of these novel macromolecules stem from the possibility of modulating certain properties, such as the glass-transition temperature, by specific structural modifications linked to the type of furanic monomer(s) used and of modifying their structure by calling upon the peculiar reactivity of the furanic heterocycle. The latter approach will be described in a forthcoming paper. Other properties of these polyurethanes, as well as more elaborate structures, are being investigated.

**Acknowledgment.** We wish to thank the FURCHIM Co. and the Agence de l'Environnement et de la Maîtrise de l'Energie (ADEME) for their financial support.

### References and Notes

- Gandini, A. In *Comprehensive Polymer Science, First Supplement*; Aggarwal, S. L., Russo, S., Eds.; Pergamon Press: Oxford, UK, 1992; p 527.
- Gandini, A. *ACS Symp. Ser.* **1989**, *433*, 195.
- Quillerou, J.; Belgacem, M. N.; Gandini, A.; Rivero, J.; Roux, G. *Polym. Bull.* **1989**, *21*, 255.

- (4) Belgacem, M. N.; Quillerou, J.; Gandini, A.; Rivero, J.; Roux, G. *Eur. Polym. J.* **1989**, *25*, 1125.
- (5) Belgacem, M. N.; Quillerou, J.; Gandini, A. *Eur. Polym. J.* **1993**, *29*, 1217.
- (6) Eckert, H.; Forster, B. *Angew. Chem.* **1987**, *99*, 922.
- (7) Cawse, J. L.; Standford, J. L.; Still, R. H. *Makromol. Chem.* **1984**, *185*, 708.
- (8) Anzuino, G.; Pirro, A.; Rossi, O.; Friz, L. P. *J. Polym. Sci. Polym. Chem.* **1975**, *13*, 1657.
- (9) Hager, W.; Ueberreiter, K. *Makromol. Chem.* **1979**, *180*, 939.
- (10) Entelis, S. G.; Nesterov, O. V. *Russ. Chem. Rev.* **1966**, *35*, 917.
- (11) Chang, M. C.; Chen, S. *J. Polym. Sci., Polym. Chem.* **1987**, *25*, 2543.
- (12) Chang, V. S.; Kennedy, J. P. *Polym. Bull.* **1983**, *9*, 479.
- (13) Yang, W. P.; Macosko, C. *Makromol. Chem., Macromol. Symp.* **1989**, *25*, 23.
- (14) Ghafari, M.; Pham, Q. T. *Makromol. Chem.* **1983**, *184*, 1669.
- (15) Cawse, J. L.; Stanford, J. L.; Still, R. H. *Br. Polym. J.* **1985**, *17*, 233.
- (16) Gandini, A.; Martinez, R. *Makromol. Chem.* **1983**, *184*, 1189.
- (17) Malichenko, B. F.; Typma, V. N.; Nestrov, A. Ye.; Shevlynakov, A. S. *Vysokmol. Soedin.* **1967**, *A9*, 2624.
- (18) Mitiakoudis, A.; Gandini, A. *Macromolecules* **1991**, *24*, 830.
- (19) Orzeszko, A.; Kolbrecki, A. *J. Appl. Polym. Sci.* **1980**, *25*, 2969.
- (20) Glawinski, S.; Pajak, Z. *Carbon* **1982**, *20*, 13.